Cancer Biology & Therapy

ISSN: (Print) (Online) Journal homepage: www.tandfonline.com/journals/kcbt20

Effect of extracellular vesicle ZNF280B derived from lung cancer stem cells on lung cancer progression

Qixia Guo, Jiayan Lu, Hui Zhao, Ding Zhou & Hua Liu

To cite this article: Qixia Guo, Jiayan Lu, Hui Zhao, Ding Zhou & Hua Liu (2025) Effect of extracellular vesicle ZNF280B derived from lung cancer stem cells on lung cancer progression, Cancer Biology & Therapy, 26:1, 2450849, DOI: 10.1080/15384047.2025.2450849

To link to this article: https://doi.org/10.1080/15384047.2025.2450849

CANCER BIOLOGY & THERAPY
2025, VOL. 26, NO. 1, 2450849
https://doi.org/10.1080/15384047.2025.2450849

Taylor & Francis
Taylor & Francis Group

RESEARCH PAPER

OPEN ACCESS Check for updates

Effect of extracellular vesicle ZNF280B derived from lung cancer stem cells on lung cancer progression

Qixia Guo[a,b*], Jiayan Lu[a,b*], Hui Zhao[a], Ding Zhou[c], and Hua Liu[a]

[a]Department of Pulmonary and Critical Care Medicine, Affiliated Hospital of Nantong University, Medical School of Nantong University, Nantong, People's Republic of China; [b]Department of Pulmonary and Critical Care Medicine, Rugao Boai Hospital, Nantong, People's Republic of China; [c]Department of Radiotherapy, LianShui County People's Hospital, Huai'an, People's Republic of China

ABSTRACT

Objective: The purpose of this research was to investigate the role of extracellular vesicles derived from lung cancer stem cells (lung CSCs-EVs) in lung cancer and to explore their potential mechanisms.

Methods: Lung CSCs were first isolated and verified using flow cytometry and RT-qPCR assays. Lung CSCs-EVs were extracted through ultracentrifugation and further characterized using transmission electron microscopy and Western blotting. The interaction between lung CSCs-EVs and lung cancer cells was observed through PKH67 staining. Subsequently, we analyzed the differentially expressed genes in lung CSCs using bioinformatics data analysis and evaluated the prognostic value of ZNF280B in lung cancer with the Kaplan-Meier Plotter. RT-qPCR was utilized to assess the mRNA expression levels of these genes, while Western blotting was used to evaluate the protein expression levels of ZNF280B and P53. Next, CCK-8 and colony formation assays were conducted to assess the effects of lung CSCs-EVs and ZNF280B on cancer cell proliferation, migration (via wound healing assay), and invasion (using transwell assay). Additionally, subcutaneous tumor-bearing experiments in nude mice were performed to evaluate the roles of lung CSCs-EVs in lung cancer progression *in vivo*.

Results: The results indicated that lung CSCs-EVs accelerated the progression of lung cancer. Mechanistically, these lung CSCs-EVs transferred ZNF280B into cancer cells, leading to the inhibition of P53 expression.

Conclusions: In summary, the manuscript first describes the molecular mechanism by which lung CSCs-EVs promote pro-cancer functions in lung cancer through the ZNF280B/P53 axis.

ARTICLE HISTORY
Received 17 August 2024
Revised 12 December 2024
Accepted 3 January 2025

KEYWORDS
Lung cancer; CSCs; extracellular vesicle; ZNF280B; P53

Introduction

According to the GLOBOCAN 2022 statistics, lung cancer ranks first in both incidence and mortality among all types of cancer. Each year, there are over 2.4 million new cases and 1.81 million deaths.[1] Non-small cell lung cancer (NSCLC) constitutes the majority of lung cancer cases.[2] Despite significant advancements in treatment, the average 5-y survival rate for NSCLC has remained at a mere 16% over the past 40 y.[3] Tumor recurrence and metastasis are considered the primary causes of adverse clinical outcomes and cancer-related deaths.[4] Furthermore, most patients with early-stage lung cancer do not exhibit clinical symptoms and are often diagnosed at advanced or metastatic stages, resulting in missed opportunities for optimal treatment.[5] Therefore, elucidating the potential mechanisms underlying malignant progression in lung cancer and identifying new therapeutic targets has significant clinical implications.

Cancer stem cells (CSCs) are a highly tumorigenic subgroup of tumor cells characterized by their ability to self-renew and differentiate in multiple directions.[6] Substantial research has demonstrated that CSCs are instrumental in tumor initiation, progression, recurrence, and treatment resistance.[7–9] Recently, attention has shifted to CSCs-EVs, which facilitate communication between CSCs and non-CSCs by delivering a variety of bioactive molecules, thereby influencing cancer progression and the surrounding microenvironment.[10] Exosomes, a type of lipid-based extracellular vesicle, transport proteins, lipids, mRNA, miRNA, and other molecules from parental cells to recipient cells, serving as important intercellular signal transducers.[11] Recent studies have identified that CSCs-EVs play a crucial role in the malignant progression of various cancers, including lung cancer. For instance, exosomal lncRNA CDKN2B-AS1 derived from CSCs has been shown to promote the occurrence and development of thyroid cancer by regulating the miR-122-5p-P4HA1 pathway.[12] Additionally, bladder CSC-mediated exosome miR-105-5p has been found to accelerate the malignancy of bladder cancer by targeting GPR12.[13] Furthermore, lung CSCs-EVs have been implicated in facilitating lung cancer the metastasis via the miR-210-3p/FGFRL1 pathway.[14] Therefore, this manuscript aims to further investigate the

CONTACT Hua Liu rgryrc@163.com Department of Pulmonary and Critical Care Medicine, Affiliated Hospital of Nantong University, Medical School of Nantong University, No. 20 Xisi Road, Chongchuan District, Nantong 226001, People's Republic of China

*These authors contributed equally to this work and share first authorship.

Supplemental data for this article can be accessed online at https://doi.org/10.1080/15384047.2025.2450849.

mechanisms by which lung CSCs-EVs contribute to the progression of lung cancer.

In this research, microarray data (GSE50627) were utilized to identify differentially expressed genes (DEGs) in lung CSCs. Among the screened DEGs, ZNF280B was selected due to its expression significantly upregulated expression. Functional experiments further confirmed the association between ZNF280B and lung cancer progression. However, it remains unclear whether ZNF280B mediates signaling communication between lung CSCs and lung cancer cells through the delivery of extracellular vesicles. Therefore, the paper aimed to investigate whether and how ZNF280B facilitates the signal communication between lung CSCs and lung cancer cells via extracellular vesicles. This study not only enhances the understanding of the regulatory pathways involving lung CSCs-EVs, but also provides new directions and potential targets for lung cancer treatment.

Materials and methods

Microarray analysis

The raw microarray data for the transcriptomic analysis of NSCLC stem cells (GSE50627) were obtained from GEO database (http://www.ncbi.nlm.nih.gov/geo). Affymetrix microarrays were performed on cancer stem cells using the GeneChip Human Gene 1.0 ST array. The dataset comprised a total of five cell samples, including a normal stem cell group (isolated from a normal lung epithelial cell line, $n = 2$) and a cancer stem cell group (isolated from A549 and NCI-H2170 cells, $n = 3$). The UALCAN database (http://ualcan.path.uab.edu/) was utilized to predict the expression of ZNF280B in lung adenocarcinoma (LUAD) and lung squamous cell carcinoma (LUSC). Subsequently, the Kaplan-Meier Plotter website (http://kmplot.com/analysis/index.php?p=background) was employed to further evaluate the association between ZNF280B expression and overall survival (OS) and first progression (FP) in lung cancer patients. Additionally, the Vesiclepedia database (http://microvesicles.org/index.html) was used to predict the presence of ZNF280 in stem cell extracellular vesicles.

Cells

Cell Bank of the Chinese Academy of Sciences (Shanghai, China) provided the human normal lung epithelial cell line BEAS-2B (Cat. No. SCSP-5067), the A549 cell line (Cat. No. SCSP-503), and the H2170 cell line (Cat. No. SCSP-5098). DMEM medium (Gibco, USA) was used to culture the BEAS-2B and A549 cells, while RPMI-1640 medium was utilized for the H2170 cells. All media were supplemented with 1% penicillin/streptomycin and 10% fetal bovine serum (FBS; Gibco). The culture conditions were maintained at 5% CO_2 and 37°C.

Enrichment of lung CSCs

A549 and H2170 spheres were enriched as previously described.[14] Specifically, A549 and H2170 cells were first prepared as single-cell suspensions and seeded onto 6-well ultra-low attachment plates (Corning, USA). The cells were cultured in serum-free stem cell medium (SCM), which was prepared using DMEM/F12K (Gibco), 10 ng/mL rhEGF (Sigma, USA), 10 ng/mL bFGF (Sigma), and 4 U/I insulin (Sigma) for 12 d, followed by dissociation with Accutase (Invitrogen, USA). The spheres after the fifth generation were used for subsequent assays.

Isolation and characterization of lung CSCs

As preceding described,[15] Lung CSCs were obtained. Briefly, $CD133^+$ cells were isolated using an immunomagnetic bead sorting kit and instrument. The cells were prepared as single-cell suspensions and incubated with a CD133 antibody-bead complex for 30 min. Subsequently, the supernatants were removed by centrifugation, and the cells were re-suspended by adding a sorting solution. Next, the cell suspensions were processed using a separation column to eluate the $CD133^+$ cells. Finally, flow cytometry was employed to sort the cells that had been incubated with either the CD133-PE antibody or the control IgG-PE antibody.

Transient transfection assay

The ZNF280B overexpression vector (ZNF280B) and the corresponding negative control vector (pcDNA3.1) were obtained from Sino Biological (Beijing, China). GenePharma (Shanghai, China) supplied the small interfering RNA specific for ZNF280B (siZNF280B) along with its corresponding negative control (siRNA). Lipofectamine 3000 (Invitrogen, USA) was used to transfect these vectors and siRNAs into A549 and H2170 cells. After 6–12 h of transfection, the medium was discarded and replaced with fresh medium, and the cells were incubated for an additional 24 or 48 h. Following transfection, subsequent experiments were conducted, and RT-qPCR was employed to assess the transfection efficiency.

Extraction and identification of lung CSCs-EVs

Lung CSCs-EVs were extracted as described by Liu et al.[16] The fifth generation of lung CSCs was transferred to serum-free medium and cultured for 12 h. Cell supernatants were harvested and centrifuged at 800 × g for 10 min, followed by a second centrifugation at 20, 000 × g for 20 min to remove cell debris. The supernatants were then filtered using a 0.22 μm filter (Millipore, USA) and subjected to centrifugation at 100, 000 × g for 90 min. The resulting pellets were re-suspended in 100 μL of PBS to obtain relatively pure lung CSCs-EVs. All procedures were performed at 4°C. A transmission electron microscope (TEM) (Hitachi, Tokyo, Japan) was used to visualize the purified lung CSCs-EVs. Western blot analysis was conducted to assess the presence of extracellular vesicle biomarkers, including CD9, CD81, TSG101 and CD63. Additionally, we measured the protein expression level of the negative control, Calnexin.

To obtain lung CSCs-EVs containing siRNA and siZNF280B, siRNA and siZNF280B were transfected into lung CSCs. After transfection 48 h, the cells were collected and centrifuged to isolate the transfected lung CSCs-EVs. In addition, fresh medium was used to replace the existing culture

medium before EVs isolation following transfection to prevent any potential confounding effects.

Extracellular vesicle labeling

Lung CSCs-EVs were labeled using a PKH67 fluorescence probe (Sigma) to observe the entry of these vesicles into lung cancer cells following co-incubation. To prevent micelle contamination, the following steps were taken. Firstly, the concentration and usage amount of the labeling reagent were strictly controlled. Precise measurement and optimization of experimental conditions were carried out to ensure that the labeling reagent functions within a reasonable range and reduce the risk of micelle formation due to excessive reagent. Secondly, environmental factors such as temperature and pH value during the labeling process were strictly monitored and adjusted. Appropriate environmental conditions can lower the possibility of micelle formation. For example, maintaining within a specific temperature range to avoid unnecessary reactions caused by excessive or low temperatures. Thirdly, multiple filtration and washing steps were performed before and after labeling. Filters with appropriate pore sizes were used to remove possible micelles and other impurities and ensure the purity of the labeling system. After incubation with PKH67-labeled lung CSCs-EVs for 3 h, cancer cells were counterstained with DAPI (Sigma). Finally, Fluorescence microscope (Carl Zeiss, Germany) was used to observe green fluorescence. In addition, to determine whether micelle contamination occurred during the labeling process, we conducted a particle size analysis on the labeled EVs. The particle size of exosomes was analyzed using the NanoSight NS300 (NanoSight Technology, Malvern, UK).

RNA extraction and rt-qPCR

Total RNAs were extracted using TRIzol reagent (Invitrogen, USA). The PrimeScript RT Reagent Kit (Takara, Japan) was utilized to synthesize complementary DNA (cDNA). The SYBR Premix Ex TaqTM (Takara) was employed to quantify RNA expression levels. The $2^{-\Delta\Delta Cq}$ method was used to assess the relative expression levels of ALDH, OCT4, NANOG, SOX2, ZNF280B and TP53, with GAPDH serving as the normalized control. Primers for ALDH, OCT4, NANOG, SOX2, ZNF280B and TP53 were obtained from GenePharma, and the sequences were seen in Table 1. In the co-incubation experiment, lung CSC-EVs were co-incubated with A549 and H2170 cells for 24 h.

Western blotting

Total proteins were extracted from lung CSCs, lung CSCs-EVs and transfected A549 and H2170 cells using the RIPA lysis buffer (Beyotime, China). The protein concentration was then determined using a BCA assay kit (Beyotime). A total of 40 μg protein samples were separated by SDS-PAGE and subsequently transferred to PVDF membranes. The membranes were incubated with primary antibodies overnight, followed by incubation with secondary antibody for 2 h. Protein bands were visualized using ECL detection reagents (Thermo, USA). The antibodies used in this study were as follows: anti-CD9 (1:1000, ab223052, Abcam), anti-CD81 (1:1000, ab109201, Abcam), anti-TSG101 (1:1000, ab228013, Abcam), anti-CD63 (1:1000, ab134045, Abcam), anti-Calnexin (1:1000, ab133615, Abcam), anti-ZNF280B (1:1000, #DF9950, Affinity Biosciences), anti-P53 (1:1000, ab131442, Abcam) and anti-GAPDH (1:2000, ab181602, Abcam).

Cell viability assay

After the treatments (transfected or co-cultured with lung CSCs-EVs), a Cell Counting Kit-8 (CCK-8) assay (Beyotime) was employed to assess cell proliferation of A549 and H2170 cells. Briefly, A549 and H2170 cells (2×10^3 cells/well) were seeded in 96-well plates and cultured for 0, 24, 48, 72 h. Subsequently, 10 μL of CCK-8 was added, and the absorbance was measured at 450 nm.

Colony formation assay

Each group of treated A549 and H2170 cells was seeded into 6-well plates. After incubation for 7 d at 37°C, the cell colonies were fixed with 4% paraformaldehyde (Sigma) and stained with 1% crystal violet (Sigma) for 10 min. The stained colonies were then photographed and counted for statistical analysis.

Wound healing assay

Following treatments (transfected or co-cultured with lung CSCs-EVs), a scratch assay was performed to assess the migratory ability of A549 and H2170 cells. In brief, the A549 and H2170 cells were plated in 6-well plates (2×10^5 cells/well) and consistent wounds were created using a pipette. Subsequently, non-adherent cells were washed with PBS, and the remaining cells were cultured in a medium containing 2% FBS. Photographs were taken at 0 hours and 24 hours, respectively (40X).

Table 1. Primers for rt-qPCR.

Targets	Sequences	
ALDH	F: 5′-TGTTAGCTGATGCCGACTTG-3′	R: 5′-TTCTTAGCCCGCTCAACACT-3′
OCT4	F: 5′-GCTCGAGAAGGATGTGGTCC-3′	R: 5′-CGTTGTGCATAGTCGCTGCT-3′
NANOG	F: 5′-TCTGGACACTGGCTGAATCCT-3′	R: 5′-CGCTGATTAGGCTCCAACCAT-3′
SOX2	F: 5′-GCCTGGGCGCCGAGTGGA-3′	R: 5′-GGGCGAGCCGTTCATGTAGGTCTG-3′
ZNF280B	F: 5′-TGAGCTAATCTTTGTTGGGGTG-3′	R: 5′-TGCAATTTGCGAGCAGTATCTTT-3′
TP53	F: 5′-CAGCACATGACGGAGGTTGT-3′	R: 5′-TCATCCAAATACTCCACACGC-3′
GAPDH	F: 5′-GAAGGTGAAGGTCGGAGTC-3′	R: 5′-GAAGATGGTGATGGGATTTC-3′

Cell invasion assay

The cell invasion was assessed using a Transwell chamber (8 μm pore size, Corning) pre-coated with Matrigel (BD Biosciences, USA). The experiments were conducted following the manufacturer's instructions. After the treatments (transfection or co-culture with lung CSCs-EVs), the invading cells were fixed at the bottom of the chamber. Subsequently, 0.1% crystal violet was applied to stain the fixed A549 and H2170 cells. Finally, the stained A549 and H2170 cells were counted and photographed using a microscope.

In vivo tumorigenesis assay

The lung cancer cell xenograft in nude mice was conducted as previously described.[17] Male BALB/c nude mice (4 weeks, 10–15 g) were obtained from the Experimental Animal Center of Nantong University (Nantong, China). Animal models were established by subcutaneously injecting A549 cells (5×10^6) into the right flanks of the BALB/c nude mice. To investigate the effects of lung CSCs-EVs on the progression of lung cancer *in vivo*, the nude mice were further injected with either lung CSCs-EVs or PBS via the tail vein. Tumor volumes were measured every 4d, and tumor volume was calculated using the formula: volume = (length × width^2/2. After 16d, all nude mice were sacrificed humanely and the subcutaneous tumors were excised for weighing and photographing. Subsequently, the ZNF280B and TP53 expression levels of tumor tissues were tested by RT-qPCR. *In vivo* experiments were conducted in accordance with the guidelines approved by the Ethics Committee of the Experimental Animal Center of Nantong University (Approval Number: S20240417–001).

Statistical analyses

All experiments were repeated three times and the data are presented as the mean ± standard deviation. All statistical analyses were performed using GraphPad Prism 8.0. Unpaired Student's t-test was used for comparisons between two groups, while one-way analysis of variance followed by Tukey's post hoc test was used for comparisons between >2 groups. The prognostic value of ZNF280B in lung cancer was assessed using Kaplan-Meier Plotter, and survival curves were compared using the log-rank test. $p < .05$ indicated a significant difference between groups.

Results

Lung CSCs-EVs promoted the proliferation, migration and invasion of lung cancer cells

Lung CSCs exhibit stem cell characteristics and express the CD133 marker.[18] Flow cytometry was utilized to isolate lung CSCs from A549 and H2170 cell lines, and the expression of CD133$^+$ was further confirmed. As illustrated in Figure 1a,b, lung CSCs were successfully separated. The expression levels of stemness-related markers, including ALDH, OCT4, NANOG, and SOX2, were subsequently assessed using RT-qPCR. The data indicated that the expression levels of these markers in CD133$^+$ A549 and CD133$^+$ H2170 were significantly higher than those in the parental A549 and H2170 cells (Figure 1c,d). To determine whether lung CSCs influence the malignant progression of lung cancer through the transfer of EVs, we co-cultured lung CSCs with lung cancer cells and observed changes in the phenotype of the malignant cells following treatment with the EV inhibitor GW4869. CCK-8 (Figure 1e,f) and clone formation (Figure 1g) experiments showed that lung CSCs can promote the proliferation ability of A549 and H2170 cells; The wound healing experiment showed that lung CSCs can promote the migration ability of A549 and H2170 cells (Figure 1h); Transwell experiments have shown that lung CSCs can promote the migration and invasion ability of A549 and H2170 cells (Figure 1i). However, adding GW4869 treatment while co culturing cells reversed the promoting effect of lung CSCs on the proliferation, migration, and invasion ability of A549 and H2170 cells (Figure 1e–i). Based on this, we believe that EVs in lung CSCs play a key role in promoting malignant progression of lung cancer cells. To further investigate the role of lung CSCs-EVs in the malignant progression of lung cancer, we extracted and characterized these vesicles. The morphology of the extracted extracellular vesicles, which ranged from 30 to 150 nm in diameter and exhibited a round structure, was observed using TEM (Figure 1j). The expression levels of specific markers for the extracted extracellular vesicles, including CD9, CD81, TSG101, and CD63, were assessed via Western Blot analysis. Additionally, we measured the protein expression level of the negative control, Calnexin (Figure 1k). Subsequently, lung CSCs-EVs labeled with PKH67 probes were co-incubated with tumor cells to determine whether these extracellular vesicles entered lung cancer cells. As shown in Figure 1l, the results indicated that lung cancer cells internalized lung CSCs-EVs, suggesting these vesicles have potential effects on lung cancer cells. In addition, we also conducted NanoSight analysis on the labeled EVs (Figure 1m). Finally, the effects of lung CSCs-EVs on the malignant cellular phenotypes of lung cancer cells were assessed. CCK-8 and colony formation assays demonstrated that the proliferation abilities of A549 and H2170 cells presented were significantly enhanced after co-incubation with lung CSCs-EVs compared to the PBS control group (Figure 1n–p). Wound healing assay, presented in Figure 1Q, indicated that lung CSCs-EVs promoted the migratory abilities of A549 and H2170 cells. Furthermore, Transwell assay revealed that lung CSCs-EVs markedly accelerated the invasion and migration of A549 and H2170 cells (Figure 1r). These findings collectively suggest that lung CSCs-EVs play an oncogenic role in lung cancer cells.

ZNF280B was enriched in lung CSCs-EVs

To elucidate the role of lung CSCs-EVs in cancer progression, we further analyzed the GSE50627 microarray dataset to screen the differentially expressed genes in lung CSCs. The volcano plot indicated that ZNF280B was significantly overexpressed in lung CSCs (Figure 2a). Then, we examined the expression levels of ZNF280B in NSCLC, which includes LUAD and LUSC, using the TCGA database. The data suggested that ZNF280B was overexpressed in cancerous tissues (Figure 2b,c). We utilized the Kaplan-Meier Plotter website to analyze the correlation

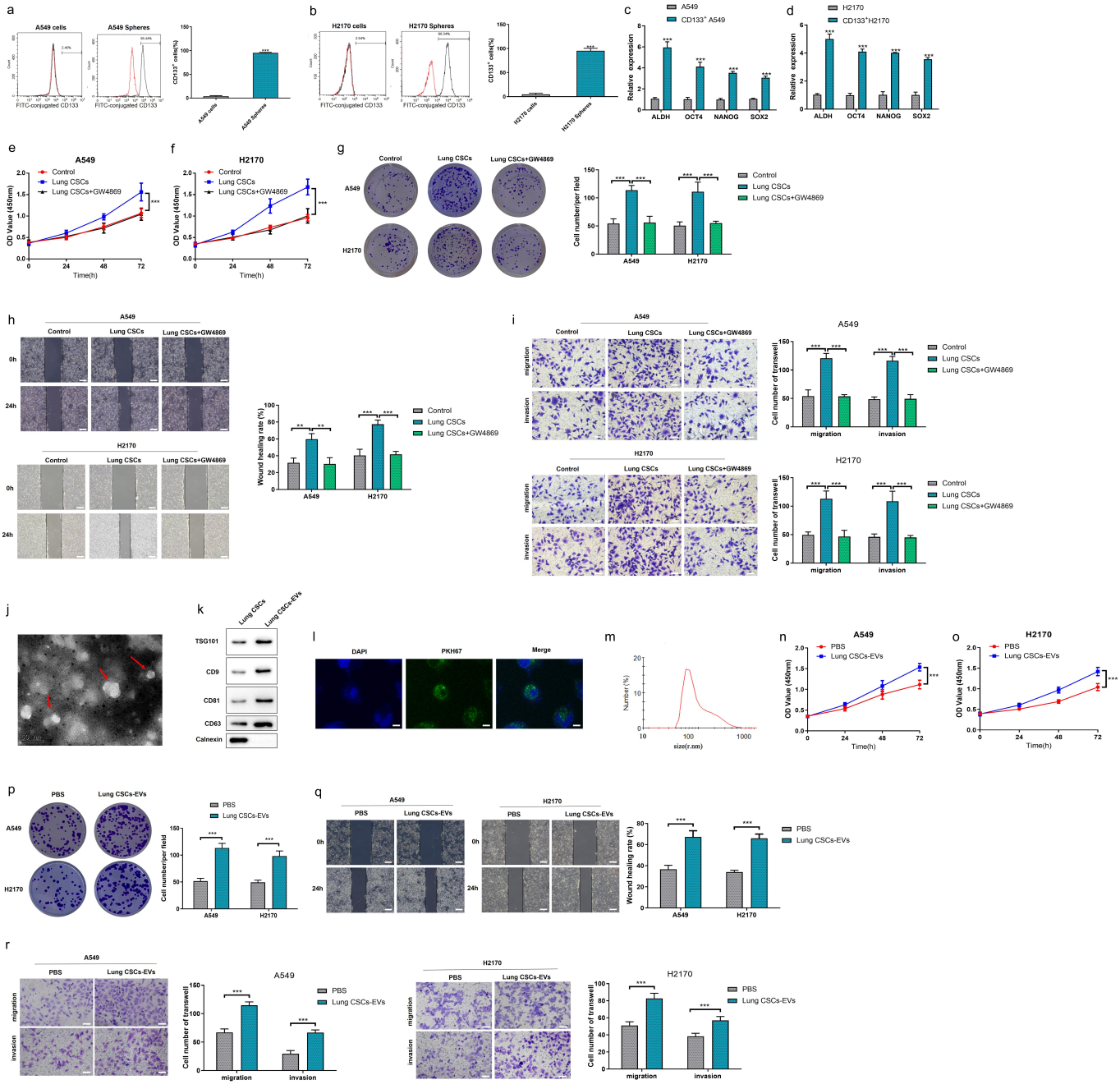

Figure 1. Lung CSCs-EVs promoted the proliferation, migration and invasion of lung cancer cells. (a-b) Lung CSCs were respectively isolated from A549 and H2170 cells using flow cytometry. (c-d) The ALDH, OCT4, NANOG and SOX2 expression levels were tested by RT-qPCR. (e-f) CCK-8 assay. (g) Colony formation assay. (h) Wound healing assay. (i) Transwell assay. (j) The morphology of lung CSCs-EVs was examined by TEM. (Scale bar: 50 nm). (k)The extracellular vesicle markers CD9, CD81, TSG101, CD63 and Calnexin protein expression levels in lung CSCs-EVs were measured by western Blot. (l) Lung CSCs-EVs were labeled with PKH67 to evaluate cellular uptake of lung cancer cells. (m) NanoSight analysis. (n-o) CCK-8 assay. (p) Colony formation assay. (q) Wound healing assay. (r) Transwell assay. ***, $P<0.001$.

between OS and FP with ZNF280B expression levels in lung cancer patients. The result indicated that the poor prognosis of lung cancer patients was closely associated with the high expression levels of ZNF280B (Figure 2d,e). Subsequently, we assessed the mRNA and protein expression levels of ZNF280B in various cell types. Compared to BEAS-2B cells, the expression levels of ZNF280B mRNA and protein were significantly elevated in A549, H2170 cells, and lung CSCs. Notably, the expression levels of ZNF280B mRNA and protein in lung CSCs were markedly higher than those in lung cancer cells (Figure 2f,g). ZNF280B expression was detected following the co-incubation of lung CSCs-EVs with A549 and H2170 cells. Similarly, the expression level of ZNF280B in lung CSCs-EVs was significantly greater than that in extracellular vesicles derived from lung cancer cells (Figure 2h). As presented in Figure 2i-k, the mRNA and protein expression levels of ZNF280B in A549 and H2170 cells were significantly up-regulated after co-incubation with lung CSCs-EVs compared to the PBS control group. Additionally, analysis

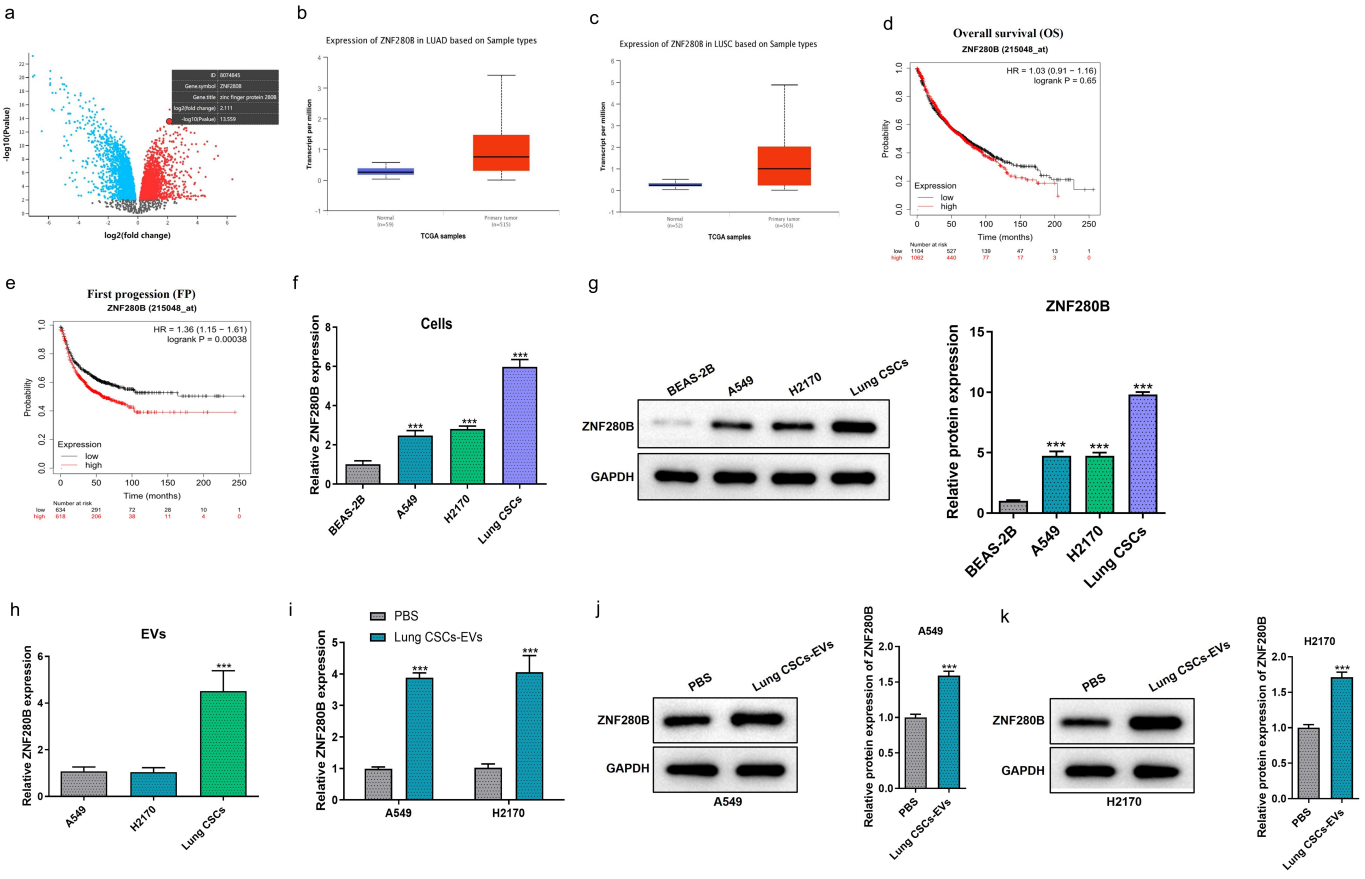

Figure 2. ZNF280B was enriched in lung CSCs-EVs. (a) The expression profile GSE50627 was bioinformatics by GEO2R online platform to screen differentially expressed genes in lung CSCs, and Volcano was drawn. (b–c)TCGA database predicted the ZNF280B expression levels in LUAD and LUSC. (d-e)Correlation analysis between ZNF280B and survival rate of lung cancer. (f-g)ZNF280B mRNA and protein expression levels in BEAS-2B, A549, H2170 cells and lung CSCs were tested by RT-qPCR and Western Blot, respectively. (h)The mRNA expression levels of ZNF280B in extracellular vesicles derived from A549 and H2170 cells, as well as lung cancer stem cells (CSCs), were analyzed using RT-qPCR. (i-k) After co-incubation with lung CSCs-EVs or PBS, the ZNF280B mRNA and protein expression levels in A549 and H2170 cells were further measured through RT-qPCR and Western Blot, respectively. ***, $P < 0.001$.

of the Vesiclepedia database indicated that ZNF280B may be present in stem cell-derived extracellular vesicles (Fig. S1). Based on these findings, lung CSCs-EVs may facilitate lung cancer progression by enriching ZNF280B.

ZNF280B stimulated the vicious phenotypes of lung cancer cells by suppressing P53 expression

Previous report has shown that ZNF280B suppresses the expression of P53 in prostate cancer.[19] Therefore, we speculated that ZNF280B may also affect P53 expression in lung cancer cells. Firstly, we utilized RT-qPCR and Western Blotting to assess the transfection efficiency of ZNF280B knockdown and overexpression in A549 and H2170 cells. As seen in Figure 3a–c, transfection with the siZNF280B significantly decreased both the mRNA and protein expression levels of ZNF280B in A549 and H2170 cells. In contrast, the mRNA and protein expression levels of ZNF280B in A549 and H2170 cells were markedly enhanced following the transfection of overexpressed ZNF280 (ZNF280B). Next, CCK-8 (Figure 3d,e), colony formation (Figure 3f), wound healing (Figure 3g), and transwell assays (Figure 3h) were performed. The data indicated that the knockdown of ZNF280B significantly reduced the proliferation, migration, and invasion capabilities of lung cancer cells. Conversely, the overexpression of ZNF280B markedly enhanced these malignant characteristics in lung cancer cells (Figure 3d-h). To confirm the pro-cancer effects of ZNF280B through the suppression of P53 expression in lung cancer, we measured the P53 protein expression levels in each cell group. As shown in Figure 3I,J, the downregulation of ZNF280B significantly increased P53 protein expression in A549 and H2170 cells, while the upregulation of ZNF280B notably decreased P53 expression. Our data revealed that ZNF280B promotes the malignant cellular phenotype of lung cancer by inhibiting P53 expression.

Knockdown of ZNF280B reversed the promoting effects of lung CSCs-EVs on the malignant phenotypes of lung cancer cells

To demonstrate that lung CSCs-EVs facilitate the progression of lung cancer by transferring ZNF280B into lung cancer cells, control siRNA and siZNF280B were transfected into lung CSCs. The data indicated that the mRNA and protein expression levels of ZNF280B in lung CSCs and CSCs-EVs were significantly decreased after the transfection of siZNF280 (Figure 4a,b). Furthermore, after A549 and H2170 cells were co-incubated with lung CSCs-EVs-siZNF280B, the mRNA and

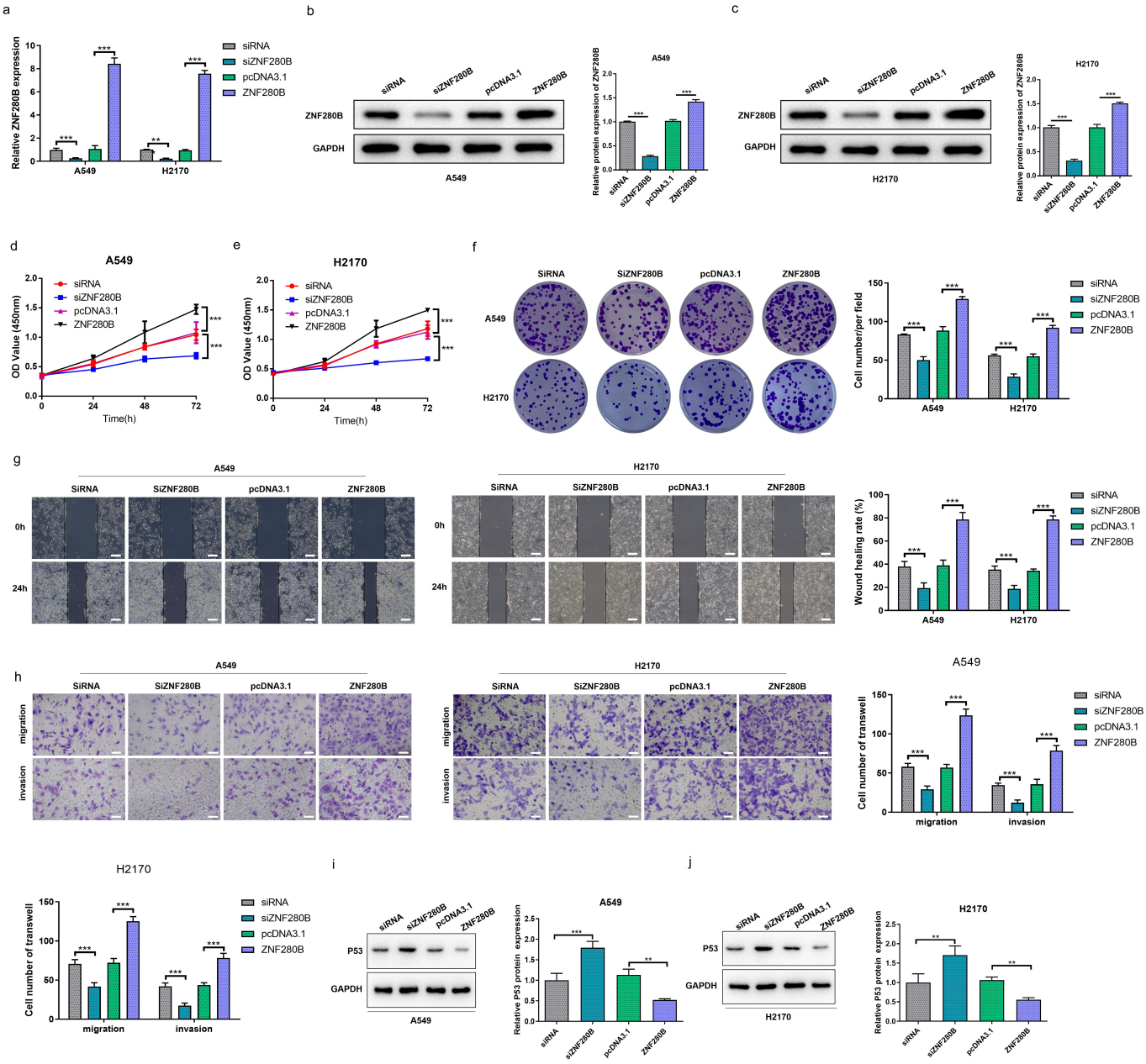

Figure 3. ZNF280B facilitated the proliferation, migration and invasion of lung cancer cells via suppressing P53 expression. (a-c) RT-qPCR and Western Blot detected the transfection efficiency of ZNF280B knockdown or overexpression in A549 and H2170 cells. (c-h) After transfection with control siRNA, siZNF280B, pcDNA3.1 or ZNF280, the proliferation, invasion and migration abilities of A549 and H2170 cells were examined by CCK-8, colony formation, wound healing and transwell experiments, respectively. (i-j)P53 expression levels in control siRNA, siZNF280B, pcDNA3.1 and ZNF280B groups of A549 and H2170 cells were tested by western Blot. **, $P<0.01$; ***, $P<0.001$.

protein expression levels of ZNF280B were markedly down-regulated (Figure 4c-e). We observed that the cell proliferation ability of lung cancer cells was significantly diminished in the lung CSCs-EVs-siZNF280B group (Figure 4f,g). Similarly, the invasion and migration abilities were impaired in the lung CSCs-EVs-siZNF280B group compared to the PBS, lung CSCs-EVs and lung CSCs-EVs-siRNA groups (Figure 4h). These findings reveal that lung CSCs-EVs exert pro-cancer functions in lung cancer cells by delivering ZNF280B.

Extracellular vesicle ZNF280B mediated by lung CSCs facilitated the progression of lung cancer in vivo

Finally, the subcutaneous tumor-bearing experiment using nude mice was conducted to evaluate the effects of extracellular vesicle ZNF280B mediated by lung CSCs on lung cancer *in vivo*. The results indicated that lung CSCs-EVs accelerated tumor growth, as evidenced by the increase in tumor volume and weight (Figure 5a-c). The mRNA and protein expression levels of ZNF280B and P53 (gene name TP53) in the tumor tissues of the model mice were further analyzed. As seen in Figure 5d,f, the mRNA and protein expression levels of

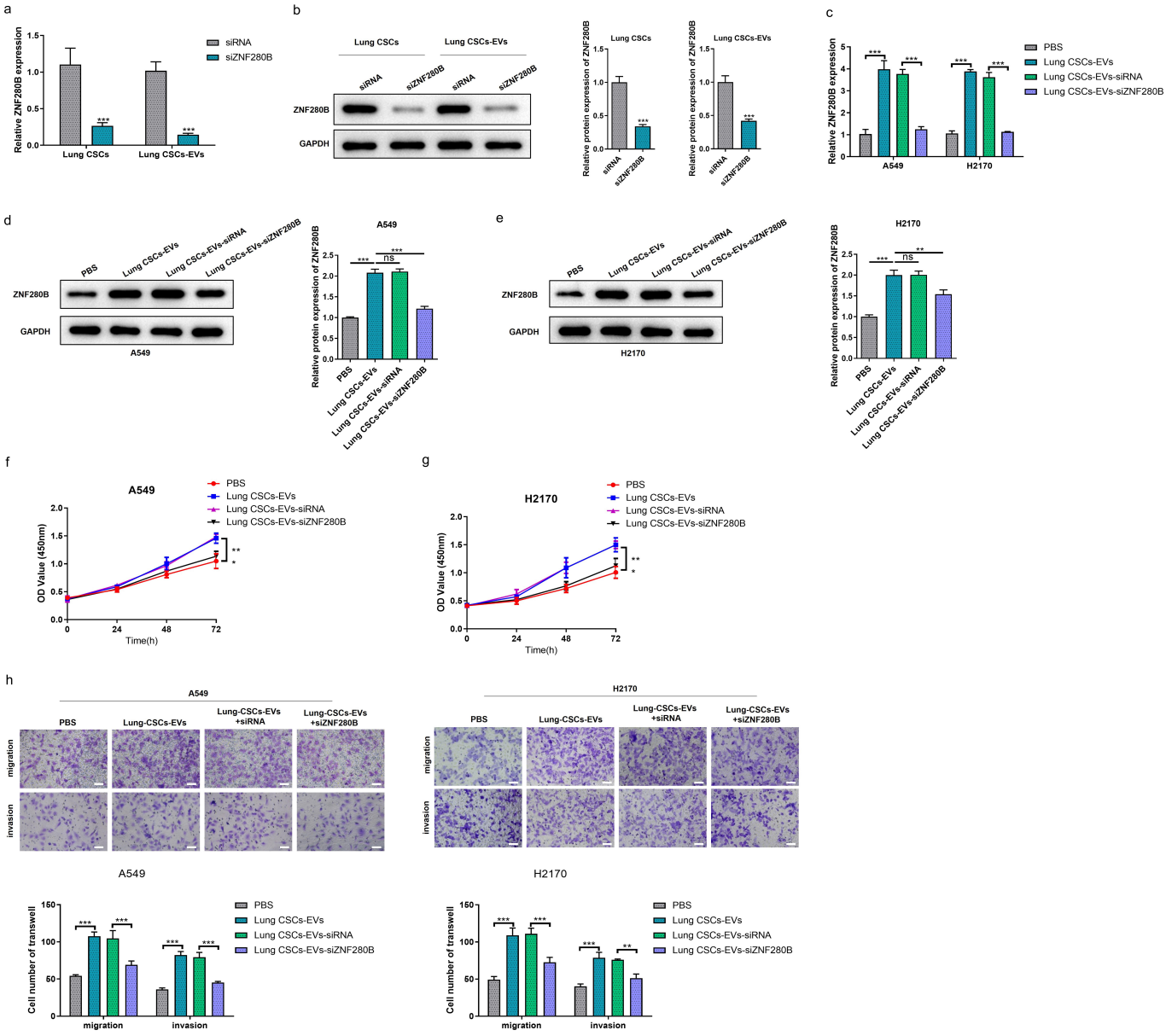

Figure 4. Knockdown of ZNF280B reversed the promoting effects of lung CSCs-EVs on the proliferation, migration and invasion of lung cancer cells. (a-b) After transfection of lung CSCs with control siRNA or siZNF208B, the mRNA and protein expression levels of ZNF280B in lung CSCs and CSC-EVs were measured. (c-e) After A549 and H2170 cells were co-incubated with PBS, lung CSCs-EVs, lung CSCs-EVs-siRNA or lung CSCs-EVs-siZNF280, the ZNF280B mRNA and protein expression levels in each group were also examined by RT-qPCR and Western Blot, respectively. (f-h) CCK-8 assay. (h) Transwell assay. **, $P < 0.01$; ***, $P < 0.001$.

ZNF280B in the experimental group (lung CSCs-EVs) were significantly elevated compared to the PBS group. Additionally, the mRNA and protein expression levels of TP53/P53 in the lung CSCs-EVs group were notably down-regulated (Figure 5e,f). These findings further demonstrate that extracellular vesicle ZNF280B derived from lung CSCs promotes lung cancer progression by down-regulating P53 expression.

Discussion

Lung cancer is a prevalent and deadly malignancy.[20] Despite significant advancements in lung cancer immunotherapy, the prognosis for patients remains suboptimal, primarily because most lung cancer cases are diagnosed at an advanced stage.[21] Consequently, identifying new therapeutic targets is essential.

Accumulated evidences have convincingly demonstrated that CSCs are pivotal to current cancer therapies. Also known as tumor initiating cells (TICs), CSCs exhibit characteristic stem cell properties.[22] They play a significant role in the onset, progression, and drug resistance of tumors. Importantly, studies have shown that extracellular vesicles facilitate communication between cancer cells and non-cancer cells, particularly between CSCs and non-CSCs, by transporting a variety of specific bioactive substances that regulate tumor progression.[6,23] In this research, we first confirmed that lung CSCs-EVs stimulated the malignant cellular phenotypes in lung cancer through functional

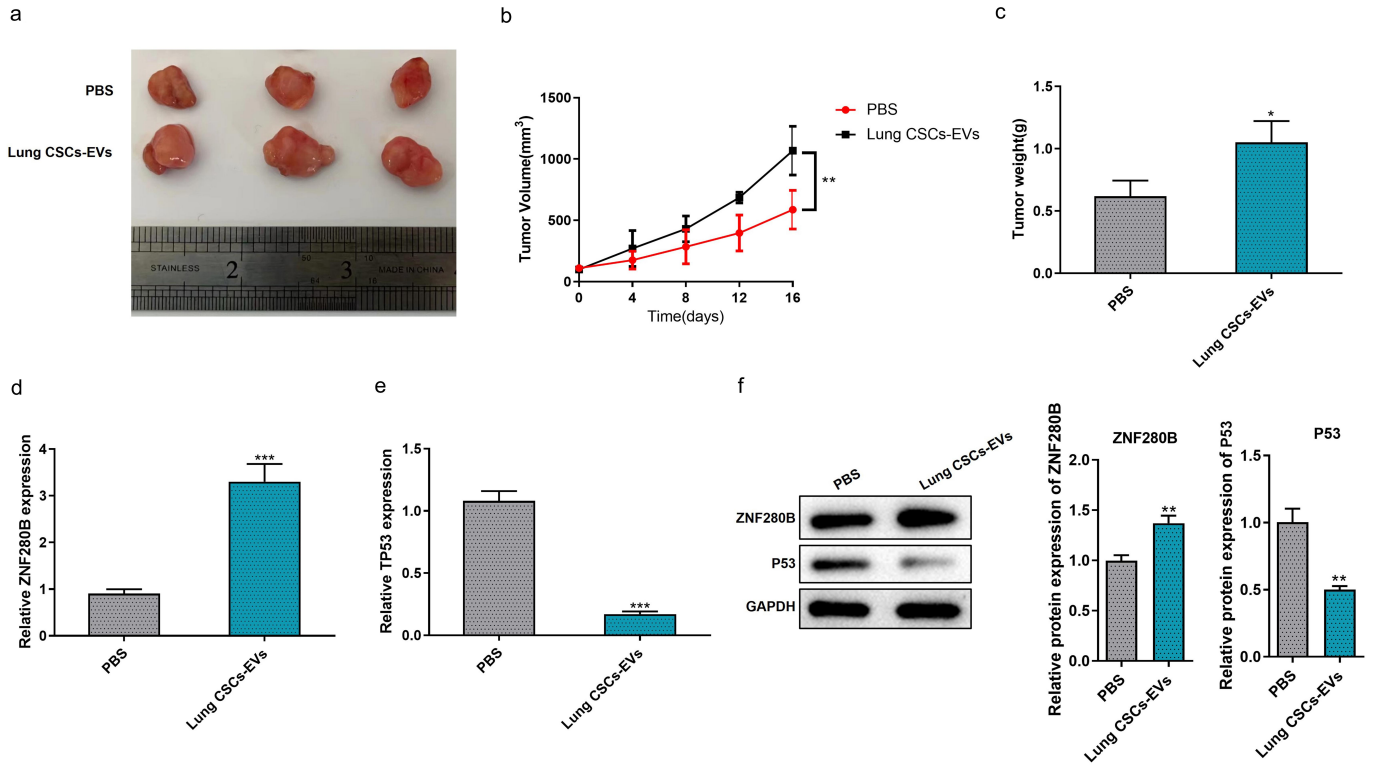

Figure 5. Extracellular vesicle ZNF280B derived from lung CSCs promoted the growth of lung cancer in vivo. (a) The transplanted tumors in nude mice were displayed. (b) The changes of tumor volume were recorded in PBS and lung CSCs-EVs groups to generate growth curve. (c) Tumor weight was measured in PBS and lung CSCs-EVs groups. (d-e) RT-qPCR was performed to examine the mRNA expression levels of ZNF280B and TP53 in PBS and lung CSCs-EVs groups. (f) Western Blot was performed to examine the protein expression levels of ZNF280B and P53 in PBS and lung CSCs-EVs groups. *, $P < 0.05$; **, $P < 0.01$; ***, $P < 0.001$.

experiments. This finding aligns with previous studies indicating that CSCs-EVs promote the metastatic phenotypes in lung cancer.[14] These results highlight the cancer-promoting role of lung CSCs-EVs in the malignant progression of lung cancer.

To further elucidate the underlying mechanisms by which lung CSCs-EVs promote lung cancer progression, we identified the significantly up-regulated gene ZNF280B in lung CSCs through bioinformatics analysis. Intriguingly, zinc finger proteins (ZNFs) constitute a large family of transcription factors that play crucial roles in DNA repair, protein degradation, transcription etc.[24] ZNFs have been reported to be abnormally expressed in various malignancies and are considered promising targets for cancer therapy. For example, ZNF831 has been shown to promote apoptosis of breast cancer cells by targeting the STAT3/Bcl2 axis.[25] Additionally, ZNF322A has been implicated in lung cancer through the transcriptional inhibition of c-Myc.[26] Our research specifically focused on the zinc finger protein 280B (ZNF280B). Previous studies have demonstrated that ZNF280B acts as an oncogene in gastric cancer[27] and prostate cancer;[19] however, its role in lung cancer remains unexplored. In this study, further analysis of TCGA and Kaplan-Meier Plotter revealed that ZNF280B is overexpressed in lung cancer and is associated with poor prognosis. Therefore, we hypothesized that ZNF280B plays a carcinogenic role in lung cancer. Our RT-qPCR results indicated that the expression levels of ZNF280B in lung CSCs were higher than those in cancer cells. Following the co-incubation of lung cancer cells with lung CSCs-EVs, the expression of ZNF280B was significantly up-regulated. Moreover, the Vesiclepedia database predicted that ZNF280B could be present in stem cell-derived extracellular vesicles. These findings suggest that lung CSCs-EVs may facilitate lung cancer progression by transferring ZNF280B into lung cancer cells. Similar regulatory patterns have also been observed in melanoma and clear cell renal cell carcinoma (CCRCC). For example, Liu et al. proposed that exosomes from melanoma stem cells transfer miR-4535 to tumor cells, thereby accelerating melanoma metastasis by suppressing the autophagy pathway.[28] Another study demonstrated that $CD103^+$ CSCs-EVs deliver miR-19b-3p into CCRCC cells, promoting CCRCC metastasis by initiating the EMT progress.[29]

It is important to note that partial ZNFs play a role in tumor progression by regulating P53 activity. Huang et al. revealed that p52-ZER6 promotes colorectal cancer progression by exacerbating P53 ubiquitination and degradation.[30] Ning et al. discovered that ZNFSNAI2 facilitates the degradation of P53 in HCT116 cells.[31] Similarly, a previous study demonstrated that ZNF280B increases P53 degradation in prostate cancer cells by inducing P53 nuclear export.[19] Consistently, we found that ZNF280B knockdown significantly elevated P53 protein levels in lung cancer cells, while ZNF280B overexpression markedly reduced P53 protein levels. Furthermore, functional experiments further indicated that ZNF280B facilitates the malignant phenotype of lung cancer cells. Our results

confirm that ZNF280B facilitates the malignant cell phenotypes of lung cancer by inhibiting P53 expression. Notably, the tumor suppressor p53 (encoded by TP53) has been shown to be relevant to the progression of various neoplasms, including lung cancer. More importantly, our study is the first to reveal that ZNF280B down-regulates P53 expression. Finally, the cell and animal experiments were conducted to clarify that lung CSCs-EVs-ZNF280B promote lung cancer progression by inhibiting P53 expression. However, due to the limited clinical resources available, we have not yet verified the ZNF280B expression and its clinical relevance in lung cancer tissues. Additionally, we will further elucidate the mechanisms by which ZNF280B downregulates p53 expression in lung cancer.

In addition, our research still has some shortcomings. For example, we identify CSCs through $CD133^{+}$. However, not all cells highly expressing CD133 are stem cells. For example, endothelial progenitor cells, which highly express CD133,[32] are not CSCs. Their main function is to participate in the repair of vascular endothelium and the formation of new blood vessels.[33] Therefore, we lacked experiments to add EPCs as negative controls. Secondly, although we have demonstrated through a series of experiments that EVs derived from lung CSCs can transfer ZNF280B to recipient cells, we still cannot determine whether this process occurs via exosomes or through cell-free extracellular/vesicular mRNA. At the same time, while Vesiclepedia indicates that ZNF280B is abundant in microvesicles, we have not conducted experiments to differentiate and analyze both exosomal and microvesicle fractions. This lack of analysis hinders our ability to gain a more comprehensive understanding of the distribution of ZNF280B. Finally, we preliminarily discovered that lung CSCs may promote cancer by delivering ZNF280B into lung cancer cells. However, we did not further demonstrate how ZNF280B is regulated in lung CSCs. When previous researchers conducted multi-omics analyses of EVs in LUAD-CSCs, they identified numerous RNA targets, including circRNAs and lncRNAs, as well as protein targets associated with ion transport, cell adhesion, and potential roles in regulating cell migration and apoptosis. These findings are relevant to cancer diagnosis and prognosis.[34] Although ZNF280B was not explicitly mentioned, the abnormal activation of tumor-related pathways associated with enriched genes-such as those involved in the extracellular matrix, ion transport, and cell adhesion and migration-may indirectly influence transcription factors or signaling networks, thereby regulating ZNF280B transcription. Alterations in the extracellular matrix and adhesion pathways can impact the binding of transcription factors to their promoters. EVs contain a variety of molecules, and proteins can indirectly modulate ZNF280B transcription by regulating pathways such as the PI3K/Akt pathway. RNA molecules, including mRNA and lncRNA, can regulate gene expression or interact with key molecules to influence their transcription. For instance, specific lncRNAs can alleviate the transcriptional inhibition of ZNF280B by miRNAs. Therefore, this necessitates further investigation.

Conclusion

Overall, this study first revealed the mechanism by which lung CSCs-EVs-ZNF280B promote lung cancer progression through the inhibition of P53 expression, offering a promising target for lung cancer therapy.

Disclosure statement

No potential conflict of interest was reported by the author(s).

Funding

This study was funded by the National Natural Science Foundation of China [Grant No. 30971306].

ORCID

Hua Liu http://orcid.org/0009-0002-1028-4687

Authors' contribution

Conception and design: Qixia Guo and Hua Liu
Data collection: Qixia Guo, Jiayan Lu, Hui Zhao
Data analysis: Qixia Guo and Ding Zhou
Writing: Qixia Guo
Supervision: Hua Liu
All authors reviewed the manuscript.

Data availability statement

Data and materials are available upon reasonable request.

Ethics approval statement

All animal experiments were conducted in accordance with ARRIVE Guidelines 2.0 and approved by the Ethics Committee of Nantong University Experimental Animal Center (Approval Number: S20240417–001).

References

1. Thai AA, Solomon BJ, Sequist LV, Gainor JF, Heist RS. Lung cancer. Lancet. 2021;398:535–554.
2. Zhou G, Pu Y, Zhao K, Chen Y, Zhang G. Heat shock proteins in non-small-cell lung cancer-functional mechanism. Front Biosci (Landmark Ed). 2023;28:56.
3. Kumar V, Yadavilli S, Kannan R. A review on RNAi therapy for NSCLC: opportunities and challenges. Wiley Interdiscip Rev Nanomed Nanobiotechnol. 2021;13:e1677.
4. Alduais Y, Zhang H, Fan F, Chen J, Chen B. Non-small cell lung cancer (NSCLC): a review of risk factors, diagnosis, and treatment. Med (Baltim). 2023;102:e32899.
5. Frydrychowicz M, Ł K, Dworacki G, Budna-Tukan J. MicroRNA in lung cancer-a novel potential way for early diagnosis and therapy. J Appl Genet. 2023;64:459–477.
6. Li X, Li X, Zhang B, He B. The role of cancer stem cell-derived Exosomes in cancer progression. STEM Cells Int. 2022;2022:9133658.
7. Khaledian B, Thibes L, Shimono Y. Adipocyte regulation of cancer stem cells. Cancer Sci. 2023;114:4134–4144.
8. Sipos FGM. Cancer stem cell relationship with pro-tumoral inflammatory microenvironment. Biomedicines. 2023;11:189.
9. Fan M, Shi Y, Zhao J, Li L. Cancer stem cell fate determination: mito-nuclear communication. Cell Commun Signal. 2023;21:159.
10. Lee NK, Kothandan VK, Kothandan S, Byun Y, Hwang SR. Exosomes and cancer stem cells in cancer immunity: current reports and future directions. Vaccines (Basel). 2021;9:441.

11. Tkach M, Théry C. Communication by extracellular vesicles: where we are and where we need to go. Cell. 2016;164:1226–1232.
12. Wu Q, He Y, Liu X, Luo F, Jiang Y, Xiang M, Zhao R. Cancer stem cell-like cells-derived exosomal lncRNA CDKN2B-AS1 promotes biological characteristics in thyroid cancer via miR-122-5p/P4HA1 axis. Regen Ther. 2023;22:19–29.
13. Pan G, Jiang B, Yi Z, Yin J, Liu Y. Exosomal miR-105-5p derived from bladder cancer stem cells targets for GPR12 to promote the malignancy of bladder cancer. BMC Urol. 2023;23:155.
14. Wang L, He J, Hu H, Tu L, Sun Z, Liu Y, Luo F. Lung csc-derived exosomal miR-210-3p contributes to a pro-metastatic phenotype in lung cancer by targeting FGFRL1. J Cell Mol Med. 2020;24:6324–6339.
15. Wang ZF, Liao F, Wu H, Dai J. Glioma stem cells-derived exosomal miR-26a promotes angiogenesis of microvessel endothelial cells in glioma. J Exp Clin Cancer Res. 2019;38:201.
16. Liu Y, Gu Y, Han Y, Zhang Q, Jiang Z, Zhang X, Huang B, Xu X, Zheng J, Cao X, et al. Tumor exosomal RNAs promote lung pre-metastatic niche formation by activating alveolar epithelial TLR3 to recruit neutrophils. Cancer Cell. 2016;30:243–256.
17. Wu J, Han X, Yang X, Li Y, Liang Y, Sun G, Wang R, Wang P, Xie S, Feng J, et al. MiR-138-5p suppresses the progression of lung cancer by targeting SNIP1. Thorac Cancer. 2023;14:612–623.
18. Sun X, Ma X, Wang J, Zhao Y, Wang Y, Bihl JC, Chen Y, Jiang C. Glioma stem cells-derived exosomes promote the angiogenic ability of endothelial cells through miR-21/VEGF signal. Oncotarget. 2017;8:36137–36148.
19. Gao S, Hsieh CL, Zhou J, Shemshedini L. Zinc finger 280B regulates sGCα1 and p53 in prostate cancer cells. PLOS ONE. 2013;8:e78766.
20. Wen T, Song L, Hua S. Perspectives and controversies regarding the use of natural products for the treatment of lung cancer. Cancer Med. 2021;10:2396–2422.
21. Wadowska K, Bil-Lula I, Ł T, M Ś-M. Genetic markers in lung cancer diagnosis: a review. Int J Mol Sci. 2020;21:21.
22. Alvina FB, Gouw AM, Le A. Cancer stem cell metabolism. Adv Exp Med Biol. 2021;1311:161–172.
23. Sun Z, Wang L, Dong L, Wang X. Emerging role of exosome signalling in maintaining cancer stem cell dynamic equilibrium. J Cell Mol Med. 2018;22:3719–3728.
24. Abbehausen C. Zinc finger domains as therapeutic targets for metal-based compounds - an update. Metallomics. 2019;11:15–28.
25. Fan J, Zhang Z, Chen H, Chen D, Yuan W, Li J, Zeng Y, Zhou S, Zhang S, Zhang G, et al. Zinc finger protein 831 promotes apoptosis and enhances chemosensitivity in breast cancer by acting as a novel transcriptional repressor targeting the STAT3/Bcl2 signaling pathway. Genes Dis. 2024;11:430–448.
26. Jen J, Liu CY, Chen YT, Wu LT, Shieh YC, Lai WW, Wang Y-C. Oncogenic zinc finger protein ZNF322A promotes stem cell-like properties in lung cancer through transcriptional suppression of c-Myc expression. Cell Death Differ. 2019;26:1283–1298.
27. Zhai J, Yang Z, Cai X, Yao G, An Y, Wang W, Fan Y, Zeng C, Liu K. ZNF280B promotes the growth of gastric cancer in vitro and in vitro. Oncol Lett. 2018;15:5819–5824.
28. Liu D, Li X, Zeng B, Zhao Q, Chen H, Zhang Y, Chen Y, Wang J, Xing HR. Exosomal microRNA-4535 of melanoma stem cells promotes metastasis by inhibiting autophagy pathway. STEM Cell Rev Rep. 2023;19:155–169.
29. Wang L, Yang G, Zhao D, Wang J, Bai Y, Peng Q, Wang H, Fang R, Chen G, Wang Z, et al. CD103-positive CSC exosome promotes EMT of clear cell renal cell carcinoma: role of remote MiR-19b-3p. Mol Cancer. 2019;18:86.
30. Huang C, Wu S, Li W, Herkilini A, Miyagishi M, Zhao H, Kasim V. Zinc-finger protein p52-ZER6 accelerates colorectal cancer cell proliferation and tumour progression through promoting p53 ubiquitination. EBioMedicine. 2019;48:248–263.
31. Kim J, Lee J, Kim U, Park JK, Um HD. Slug promotes p53 and p21 protein degradation by inducing Mdm2 expression in HCT116 colon cancer cells. Oncol Lett. 2021;22:681.
32. Rakkar K, Kadir RRA, Othman OA, Sprigg N, Bath PM, Bayraktutan U. Comorbidities and angiogenic regulators affect endothelial progenitor cell subtype numbers in a healthy volunteer control group. STEM Cell Rev Rep. 2024;20:2336–2344.
33. Garbuzova-Davis S, Boccio KJ, Ehrhart J, Sanberg PR, Appel SH, Borlongan CV. Detection of endothelial cell-associated human DNA reveals transplanted human bone marrow stem cell engraftment into CNS capillaries of ALS mice. Brain Res Bull. 2021;170:22–28. doi:10.1016/j.brainresbull.2021.01.020.
34. Luo HT, Zheng YY, Tang J, Shao LJ, Mao YH, Yang W, Yang X-F, Li Y, Tian R-J, Li F-R, et al. Dissecting the multi-omics atlas of the exosomes released by human lung adenocarcinoma stem-like cells. NPJ Evidence Med. 2021;6:48.